

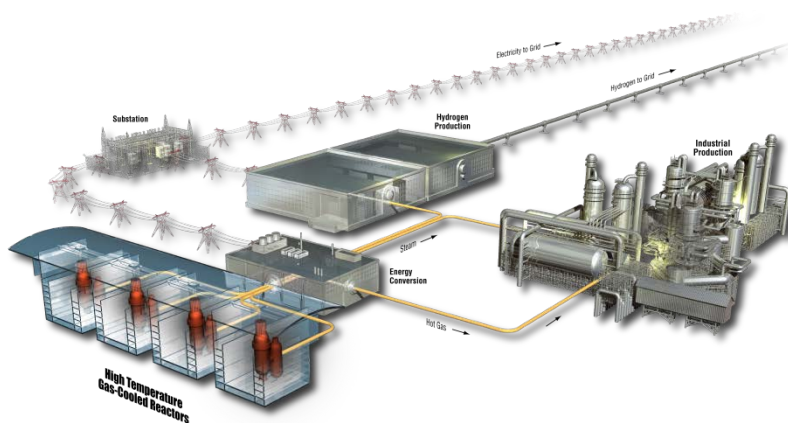
Report on the FY18 Creep Rupture and Creep-Fatigue Tests on the First Commercial Heat of Alloy 709

Project No. 23747, 29412

Michael McMurtrey

August 2018

The INL is a
U.S. Department of Energy
National Laboratory
operated by
Battelle Energy Alliance



DISCLAIMER

This information was prepared as an account of work sponsored by an agency of the U.S. Government. Neither the U.S. Government nor any agency thereof, nor any of their employees, makes any warranty, expressed or implied, or assumes any legal liability or responsibility for the accuracy, completeness, or usefulness, of any information, apparatus, product, or process disclosed, or represents that its use would not infringe privately owned rights. References herein to any specific commercial product, process, or service by trade name, trade mark, manufacturer, or otherwise, does not necessarily constitute or imply its endorsement, recommendation, or favoring by the U.S. Government or any agency thereof. The views and opinions of authors expressed herein do not necessarily state or reflect those of the U.S. Government or any agency thereof.

Report on the FY18 Creep Rupture and Creep-Fatigue Tests on the First Commercial Heat of Alloy 709

Michael McMurtrey

August 2018

**Idaho National Laboratory
INL ART Program
Idaho Falls, Idaho 83415**

<http://www.inl.gov>

**Prepared for the
U.S. Department of Energy
Office of Nuclear Energy
Under DOE Idaho Operations Office
Contract DE-AC07-05ID14517**

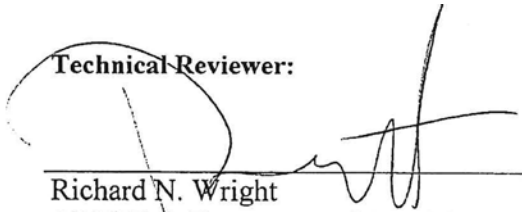
INL ART Program

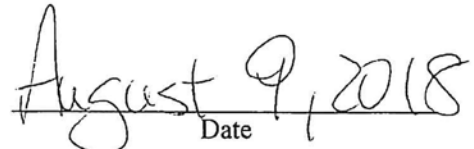
**Report on the FY18 Creep Rupture and Creep-Fatigue
Tests on the First Commercial Heat of Alloy 709**

**INL/EXT-18-46140
Revision 0**

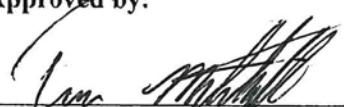
August 2018

Technical Reviewer:

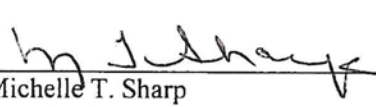

Richard N. Wright
ART High-Temperature Materials Lead

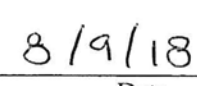

Date

Approved by:


Travis R. Mitchell
ART Project Manager


Date


Michelle T. Sharp
INL Quality Engineer


Date

ABSTRACT

Creep, fatigue, and creep-fatigue tests were performed on the commercial scale G.O. Carlson plate of Alloy 709 (ID 58776-4). The Alloy 709 heat was first processed using the argon oxygen decarburization process (AOD). A portion of the heat was then refined using electro-slag remelting (ESR). Finally, a portion of the ESR ingot underwent a homogenization heat treatment (ESR+HOMO). The three ingots were hot rolled into plates and each was further divided into three sections for different solution annealing temperatures (1050, 1100 and 1150°C). The effects of processing method and solution annealing temperature were studied in FY-18 to inform best procedures for the second heat. The solution annealing temperature of 1050°C was found to be unacceptable due to the grain size being smaller than allowed by the specifications. This material also had generally poor creep properties. Annealing at 1100 and 1150°C resulted in material with grain size that met the specifications. Both argon oxygen decarburization and electro-slag remelting were found to have desirable properties, and the homogenization heat treatment was found not significantly to improve mechanical properties.

ACRONYMS

ANL	Argonne National Laboratory
AOD	argon oxygen decarburization
ART	Advanced Reactor Technologies
ASME	American Society of Mechanical Engineers
ASTM	ASTM, International (formerly, the American Society for Testing and Materials)
ATS	Applied Test Systems
ESR	electro-slag remelting
HOMO	homogenized
INL	Idaho National Laboratory
LVDT	linear variable differential transformer
S/A	solution anneal

CONTENTS

ABSTRACT.....	v
ACRONYMS.....	vii
1. INTRODUCTION.....	1
2. EXPERIMENTAL PROCEDURE.....	1
3. RESULTS.....	2
3.1 Creep Rupture Results	2
3.2 Fatigue and Creep-Fatigue Results	5
3.3 Combined Properties.....	8
4. SUMMARY	8
5. FUTURE WORK	8
6. ACKNOWLEDGMENTS.....	9
7. REFERENCES	9

FIGURES

Figure 1. Creep curves for all preliminary 709 creep testing of the heat 58776-4.....	3
Figure 2. Example of a ruptured creep specimen. This is from the AOD S/A 1150°C plate.	3
Figure 3. Example micrographs of the AOD S/A 1050°C plate. Grain distribution was bimodal, with both large grains and very small grains present.....	4
Figure 4. Example micrograph of the AOD S/A 1100°C plate. Grains were generally uniform in size.....	4
Figure 5. Example micrographs of the AOD S/A 1150°C plate. In general, grains were uniform in size, with the occasional large grain as seen in the left micrograph.	5
Figure 6. Examples of hysteresis loops. Fatigue (left) and creep-fatigue (right) mid-life hysteresis loops of the 709 plates in the S/A 1100°C condition.....	6
Figure 7. Fatigue (a,c,e) and creep-fatigue (b,d,f) curves for the S/A 1050°C (a,b), 1100°C (c,d) and 1150°C (e,f) conditions.....	7

TABLES

Table 1. G.O. Carlson alloy 709 plate composition, as measured from the AOD plate.	1
Table 2. Summary of creep results for the preliminary creep testing of the heat 58776-4.	2
Table 3. Fatigue and creep-fatigue summary for Carlson alloy 709 testing.	6
Table 4. Summary of all mechanical testing. Replicate tests are averaged to one value.	8

Report on the FY18 Creep Rupture and Creep-Fatigue Tests on the First Commercial Heat of Alloy 709

1. INTRODUCTION

Previous work on advanced austenitic steels led to the selection of Alloy 709 for development as an available fast-reactor structural material.¹ Alloy 709 is a 25Cr 20Ni austenitic stainless steel similar to Type 316, but with improved elevated-temperature properties. The improved properties have the potential to improve the economics of the reactor by allowing for longer component lifetimes and less required component thickness. Following the down selection to Alloy 709, a number of laboratory-scale heats of the alloy were made to refine processing conditions and heat treatments to obtain the desired high-temperature mechanical properties.^{2,3,4,5,6,7,8,9} Based on these results, an industrial-scale heat of Alloy 709 was commissioned from G.O. Carlson. The composition of the heat is shown in Table 1.

Table 1. G.O. Carlson alloy 709 plate composition, as measured from the AOD plate.

	C	Mn	Si	P	Cr	Ni	Mo	N	Cb	Ti	Cu	Co	Al	B	Fe
Composition (wt%)	0.07	0.91	0.44	0.014	19.93	24.98	1.51	0.148	0.26	0.04	0.06	0.02	0.02	0.0045	Bal.

The G.O. Carlson heat (58776-4) was divided into nine smaller portions, each with a unique processing history. Three processing procedures were applied: argon oxygen decarburization (AOD), electro-slag remelting (ESR) and homogenized after the ESR process (ESR+HOMO). Each of these was solution annealed (S/Aed) at three different temperatures (1050°C, 1100°C and 1150°C), resulting in the desired nine plates with unique processing histories. The AOD process is common in steelmaking as the first step in alloy melting. The addition of an ESR step has become common commercial practice and is thought to better control impurity content in some circumstances, but the additional processing step adds to cost. High temperature homogenization was carried out to reduce segregation in the ESR ingot prior to rolling in the hope that this would reduce banding in the microstructure after solution treatment. The range of solution annealing temperatures was selected because it is thought that a 100°C temperature range is consistent with commercial practice.

Creep and cyclic testing was carried out to characterize the creep, fatigue, and creep-fatigue behavior of each processing condition for the Carlson Alloy 709 heat. The cyclic testing was conducted primarily at a single fatigue and creep-fatigue condition, which was at 650°C and 1.0% total strain ($\pm 0.5\%$ strain). For creep-fatigue, a 30-minute hold time at peak tensile strain was introduced. Creep testing was performed at 600°C with 330 MPa applied stress. The goal of this work was to determine the allowable methods of producing alloy 709 for use in the proposed American Society of Mechanical Engineers (ASME) Boiler and Pressure Vessel Code Case.

2. EXPERIMENTAL PROCEDURE

Fatigue and creep-fatigue tests at 650°C, primarily at 1.0% total strain and a 30-minute peak tensile-strain hold (creep-fatigue only), were conducted on specimens from each of the nine plate conditions. Fully reversed, strain-controlled, low-cycle triangular waveform fatigue and creep-fatigue testing were conducted at a strain rate of $10^{-3}/s$ in laboratory air using servo-hydraulic test frames in accordance with PLN-3346.¹⁰ The creep-fatigue tests followed a similar waveform as the standard fatigue test, with the addition of a strain-controlled hold time at peak tensile strain. Cycles to failure, N_f , is defined as a decrease in the peak tensile stress of 25% from the point at which the peak stress initially deviates from a steadily declining value. Creep and creep-fatigue testing followed ASTM, International, Standards E606 and E2714, respectively.^{11,12}

Creep rupture testing was performed at 600°C and 330 MPa in Applied Test Systems (ATS) creep frames. Testing was typically performed on creep frames with a 20:1 lever arm that multiplied the applied load onto the specimen, allowing for the high applied stresses. All creep testing was performed in accordance with PLN-3386.¹³ During the test, specimen elongation was measured with an extensometer connected to linear variable differential transformers (LVDTs) or to Heidenhain displacement length gauges. Following the specimen rupture, a time to rupture was recorded (time elapsed since the start of test) and the specimen length and diameter were measured and compared to pretest measurements to determine actual elongation and reduction in area, in accordance with ASTM E139.¹⁴

3. RESULTS

3.1 Creep Rupture Results

A total of 18 creep tests were performed for this preliminary study, two at each of the processing conditions and S/Aing temperatures. Test conditions were determined so that the expected creep rupture life was 1000 hours, based on previous work. Five of these tests are ongoing, as of the date of this report. These results are summarized in Table 2, with the creep curves shown in Figure 1. Specimens generally were found to rupture in the center of the gauge, as shown in the example specimen in Figure 2.

Table 2. Summary of creep results for the preliminary creep testing of the heat 58776-4.

Processing condition	S/A	Temp, C	Stress, MPa	Rupture time, hr	Strain (extensometer), %	Strain (post-test measurement), %	Reduction in area, %
AOD	1050	600	330	701	12.83	14.06	17.77
		600	330	638	11.12	12.77	16.52
	1100	600	330	1785	14.56	17.38	24.45
		600	330	1626	15.61	18.54	23.08
	1150	600	330	2712	18.87	21.54	29.46
		600	330	3296	12.37	15.74	24.67
ESR	1050	600	330	1538	30.99	26.17	44.07
		600	330	1589	29.87	25.36	38.03
	1100	600	330	2386	21.12	21.32	33.90
		600	330	ONGOING			
	1150	600	330	ONGOING			
		600	330	ONGOING			
ESR+HOMO	1050	600	330	745	13.23	13.50	18.21
		600	330	668	12.33	13.07	17.82
	1100	600	330	2274	19.86	20.89	30.51
		600	330	ONGOING			
	1150	600	330	2896	11.02	15.49	25.42
		600	330	ONGOING			

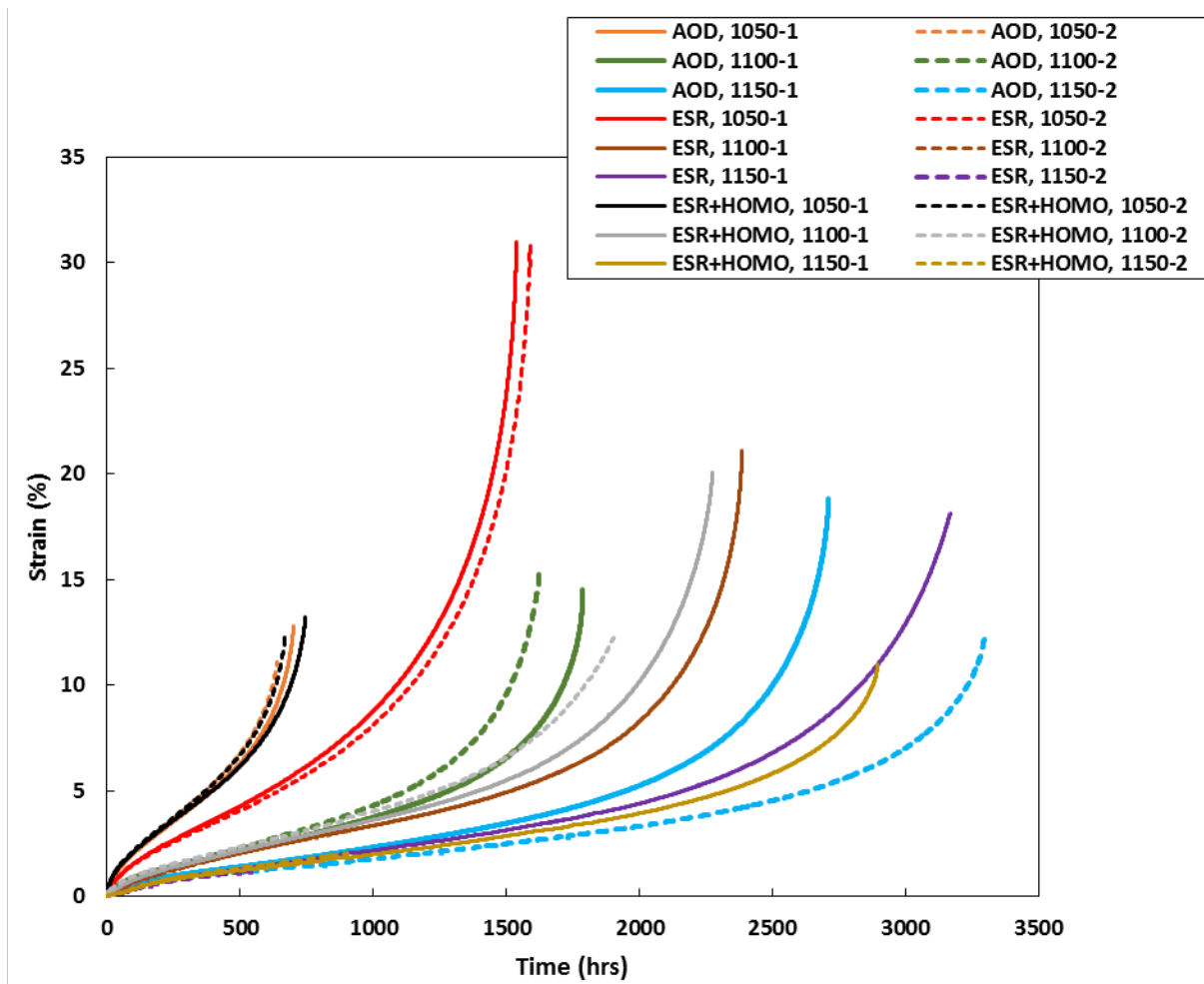


Figure 1. Creep curves for all preliminary 709 creep testing of the heat 58776-4.



Figure 2. Example of a ruptured creep specimen. This is from the AOD S/A 1150°C plate.

In general, the differences between the processing conditions (AOD vs. ESR. vs. ESR+HOMO) are minor, with the exception of ESR at the 1050°C condition. ESR S/A 1050°C was found to have a much longer than expected rupture life and also to exhibit higher total elongation. The reason for the unexpected behavior is not clear at this time, but is being examined to determine whether the cause is microstructural based.

The variation in creep properties with S/A temperatures is as expected. Creep properties tend to be poorer with decreasing grain size. The grain size is related to the S/A temperature. Higher annealing temperature results in larger grains. As an example of this, the grain size of AOD S/A 1050°C was found to be 23.9 μm on average. At S/A 1100°C, it was 31.7 μm and at S/A 1150°C, it was 39.4 μm on average. It is important to note that at the AOD S/A 1050°C condition, there was a bimodal grain distribution of very large (~800 μm) and very small grains (~20 μm), with about 60% of the surface area examined made up of large grains. The grain size distribution was fairly uniform for the S/A 1100°C condition, as well as the S/A 1150°C condition, though there were isolated large grains observed in the S/A 1150°C condition (~20% of the surface area examined was made up of large grains). Example micrographs of the three S/A temperatures are depicted in Figure 3, Figure 4 and Figure 5. Similar grain-size increases with increasing S/A temperatures are expected for ESR and ESR+HOMO, though an in depth characterization was not performed.

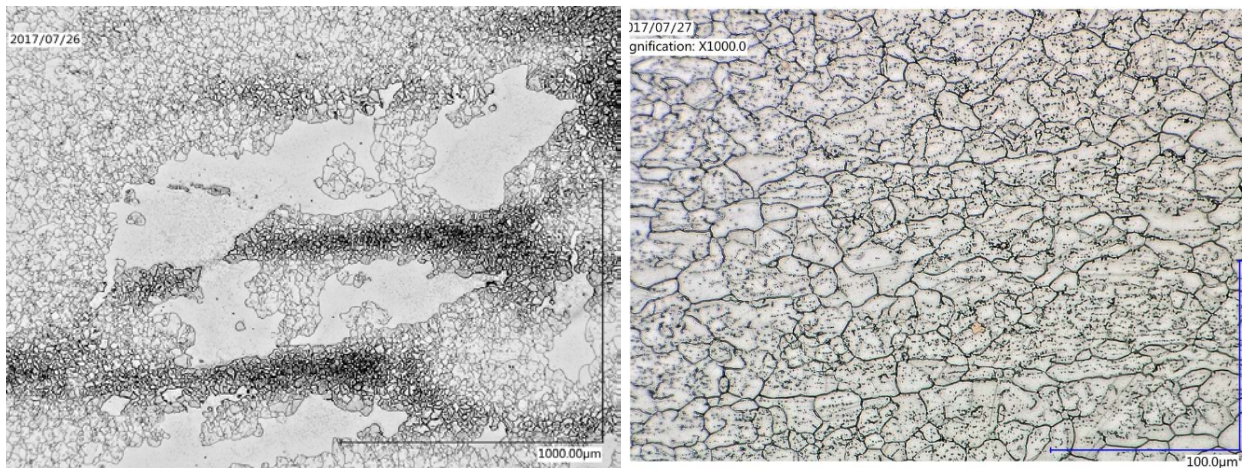


Figure 3. Example micrographs of the AOD S/A 1050°C plate. Grain distribution was bimodal, with both large grains and very small grains present.

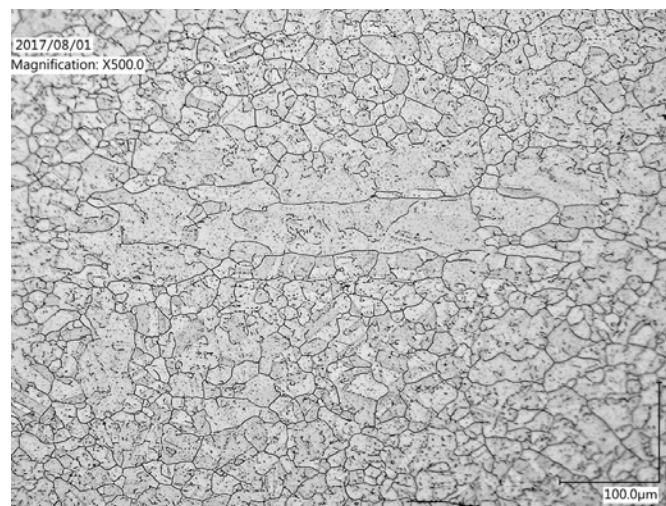


Figure 4. Example micrograph of the AOD S/A 1100°C plate. Grains were generally uniform in size.

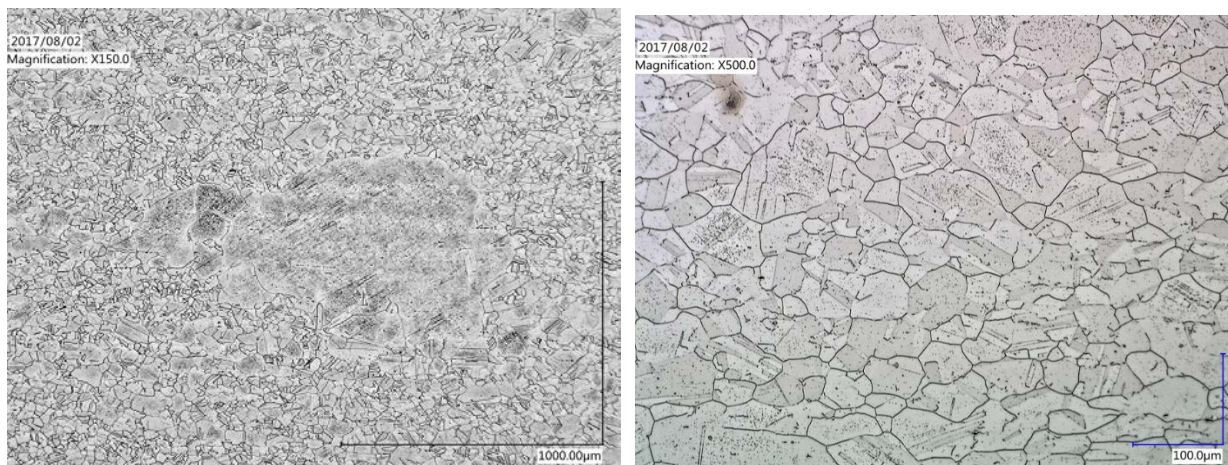


Figure 5. Example micrographs of the AOD S/A 1150°C plate. In general, grains were uniform in size, with the occasional large grain as seen in the left micrograph.

3.2 Fatigue and Creep-Fatigue Results

A total of 12 fatigue and 12 creep-fatigue tests were performed at Idaho National Laboratory (INL) on the heat 58776-4 plate of Alloy 709. This includes replicate tests performed for each AOD S/A condition, and single tests for the ESR and ESR+HOMO conditions. All testing has been completed, and the results are summarized in Table 3. Example mid-life hysteresis loops are shown in Figure 6, and all fatigue/creep-fatigue curves are shown in Figure 7.

The results of the fatigue testing exhibit some scatter. ESR, however, consistently has the poorest fatigue life at each condition tested, although in some cases, particularly the S/A 1150°C, the difference is negligible, given the expected scatter in fatigue testing (note the large difference in life between the replicate AOD tests, particularly at the S/A 1150°C condition). AOD and ESR+HOMO are similar, except in the S/A 1100°C case, where the AOD plate was found to have significantly better fatigue life. Fatigue life is expected to be inversely related to grain size (smaller grains perform better), so the results are expected to follow an opposite trend compared to the creep results. This is not always the case in the tests performed here, however. ESR had a similar fatigue life across all three S/A temperatures. ESR+HOMO was the only condition that had the best fatigue life from the S/A 1050°C condition.

Creep-fatigue life is significantly shorter than fatigue life, as expected due to the creep damage occurring during the 30 minute tensile hold. For the AOD plate, the fraction of creep-fatigue to fatigue life remains fairly constant around 0.25 at all three S/A temperatures. For ESR, this fraction is slightly higher, around 0.30, except for the S/A 1150°C condition, which drop to 0.19. ESR+HOMO has the highest fraction at S/A 1050 and 1100°C (~0.50), but drops severely at S/A 1150°C to 0.14. The severe drop for ESR and ESR+HOMO at S/A 1150°C is undesirable.

Table 3. Fatigue and creep-fatigue summary for Carlson alloy 709 testing.

Processing condition	S/A	Temp.	Strain Rate	Hold time (t_h)	Total strain ($\Delta\epsilon_t$)	Cycles to Failure
	(°C)	(°C)	(/s)	(min)	(%)	(N_{25})
AOD	1050	650	0.001	0	1.0	1683
		650	0.001	0	1.0	1440
		650	0.001	30	1.0	454
		650	0.001	30	1.0.	422
	1100	650	0.001	0	1.0	1760
		650	0.001	0	1.0	1717
		650	0.001	30	1.0	497
		650	0.001	30	1.0.	367
	1150	650	0.001	0	1.0	1954
		650	0.001	0	1.0	1391
		650	0.001	30	1.0	343
		650	0.001	30	1.0.	462
HOMO	1050	650	0.001	0	1.0	1850
		650	0.001	30	1.0.	519
	1100	650	0.001	0	1.0	1323
		650	0.001	30	1.0.	438
	1150	650	0.001	0	1.0	1458
		650	0.001	30	1.0.	281
ESR+HOMO	1050	650	0.001	0	1.0	1150
		650	0.001	30	1.0.	568
	1100	650	0.001	0	1.0	1058
		650	0.001	30	1.0.	534
	1150	650	0.001	0	1.0	1318
		650	0.001	30	1.0.	184

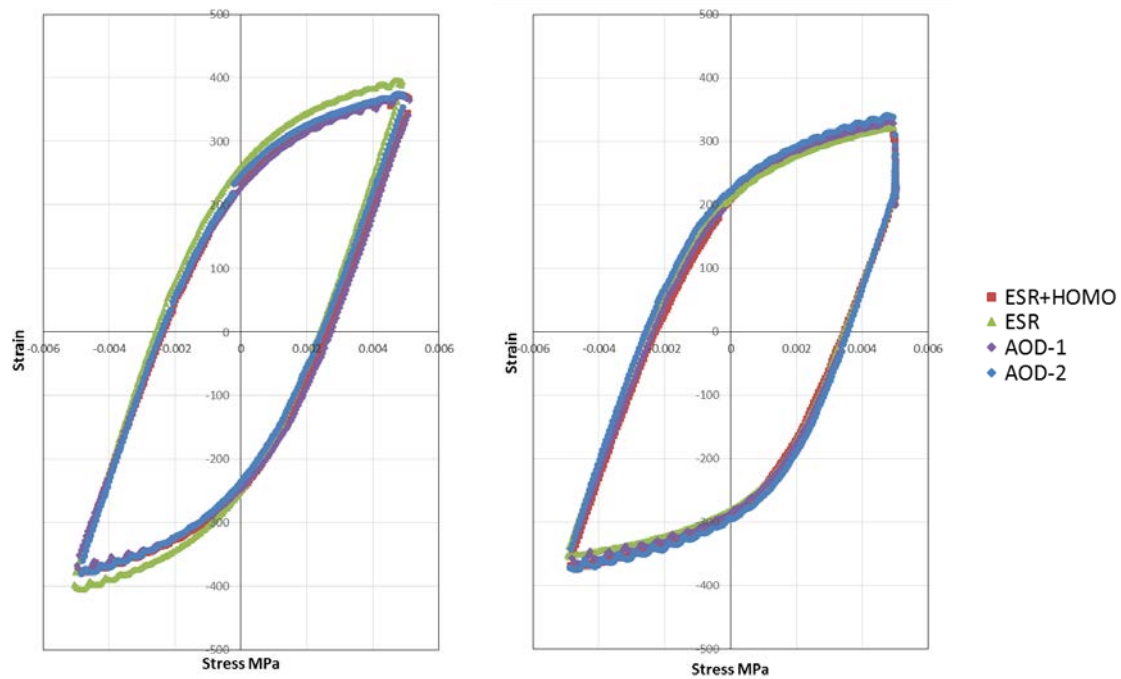
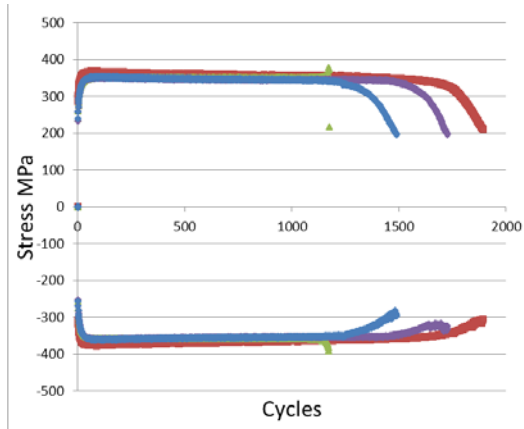
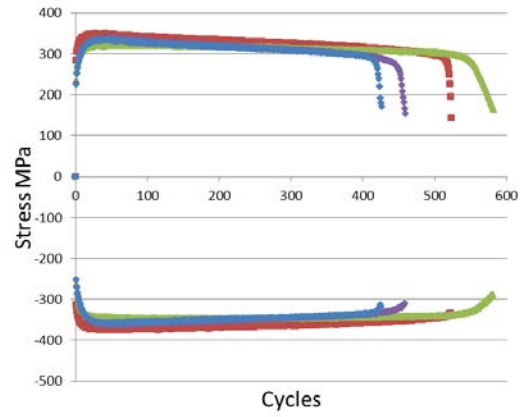


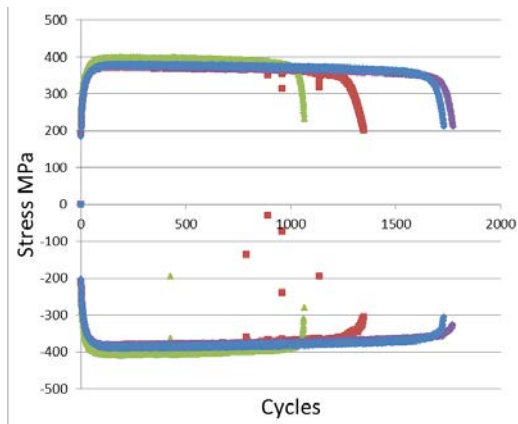
Figure 6. Examples of hysteresis loops. Fatigue (left) and creep-fatigue (right) mid-life hysteresis loops of the 709 plates in the S/A 1100°C condition.



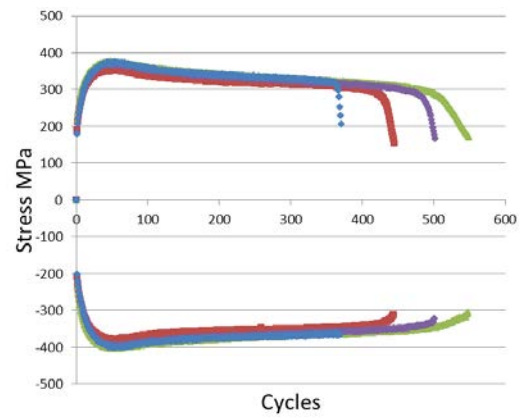
(a)



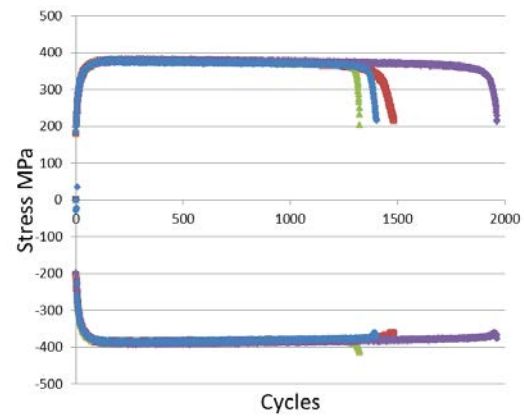
(b)



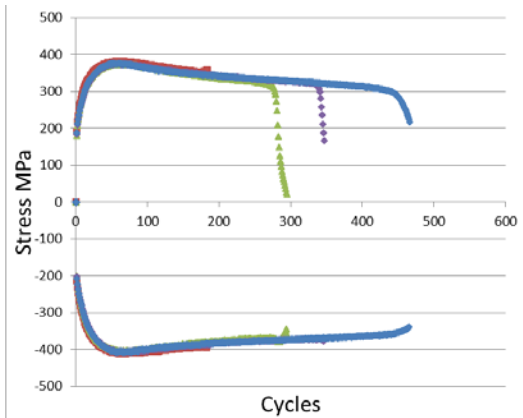
(c)



(d)



(e)



(f)

Figure 7. Fatigue (a,c,e) and creep-fatigue (b,d,f) curves for the S/A 1050°C (a,b), 1100°C (c,d) and 1150°C (e,f) conditions.

3.3 Combined Properties

Determining best processing practices is complicated by the need to balance multiple properties. Creep and fatigue, in particular, tend to be affected by processing conditions in opposite directions with respect to the S/A temperature. Table 4 summarizes all the results from the previous sections, with replicate tests being averaged into one value. While there are no creep tests finished for the ESR S/A 1150°C condition, it appears, based on Figure 1, that the life will be similar to the other conditions (around 3300 hours for ESR 1150-1). Based on creep alone, the ESR condition appears superior. However, ESR had the poorest fatigue results. Creep-fatigue at 1150°C was also particularly bad for ESR, although it should be taken into consideration that there were no replicate tests performed for ESR or ESR+HOMO for fatigue or creep-fatigue, so it is not possible to know if these values are reproducible. AOD and ESR+HOMO had similar creep properties, but the ESR+HOMO tended to do poorly in fatigue and creep-fatigue at S/A temperatures above 1050°C.

Table 4. Summary of all mechanical testing. Replicate tests are averaged to one value.

	Average Life								
	Creep (hrrs)			Fatigue (cycles)			Creep-Fatigue (cycles)		
Plate	S/A 1050°C	S/A 1100°C	S/A 1150°C	S/A 1050°C	S/A 1100°C	S/A 1150°C	S/A 1050°C	S/A 1100°C	S/A 1150°C
ADD	670	1706	3004	1562	1739	1673	438	432	403
ESR	1564	2386	Ongoing	1150	1058	1318	568	534	184
ESR+HOMO	707	2274	2896	1850	1323	1458	519	438	281

4. SUMMARY

Nine processing conditions and S/A temperature combinations of Alloy 709 were used to perform creep, fatigue, and creep-fatigue tests. In general, the lower S/A temperature (1050°C) had poor creep performance, with the exception of the ESR processing condition. The high-temperature S/A condition (1150°C) tended to have poor creep-fatigue life, with the exception of the AOD plate. The ESR plate has the best creep life, and the AOD plate tended to have the best fatigue life. The AOD or the ESR plates may be considered for future testing and, eventually, code qualification; however, there does not seem to be any substantial benefit gained by performing the addition homogenization processing step. Therefore, given that it is also an added expense when making the plate, there does not seem to be any benefit for progressing testing on the ESR+HOMO condition.

5. FUTURE WORK

Additional microstructural analysis will be performed on all plates and tested specimens. Current microstructural analysis has shown that the 1050°C S/A condition creates grains that are too small and fall outside of allowable grain sizes for this material. This restricts allowable S/A temperatures to just a 50°C window (1100–1150°C). Additional heat treatments performed at INL on portions of the AOD as-rolled plate were performed at 1075 and 1175°C, with the goal of extending the allowable S/A temperature window to 100°C (1075–1175°C). Testing similar to that described in this report will be carried out on material given those heat treatments. An additional plate was solution annealed at 1150°C to compare the lab heat treatments performed at INL with the original G.O. Carlson AOD S/A 1150°C plate.

The data generated by INL, including the five remaining creep tests that are ongoing, will be combined with testing data from Oak Ridge National and Argonne National Laboratories. The additional test data will supplement the current testing results and allow for a final decision to be made on desired processing conditions to be moved forward for additional testing.

6. ACKNOWLEDGMENTS

The research was sponsored by the U.S. Department of Energy, under Contract No. DE-AC02-06CH11357 with Argonne National Laboratory, managed and operated by UChicago Argonne LLC. Programmatic direction was provided by the Office of Nuclear Energy.

The author gratefully acknowledges the support provided by Alice Caponiti, Director, Office of Advanced Reactor Technologies (ART), Sue Lesica, Federal Manager, ART Advanced Materials Program, Robert Hill of Argonne National Laboratory, National Technical Director, ART Fast Reactors Campaign, and Sam Sham of Argonne National Laboratory, ART Technology Area Lead on Advanced Materials.

The author acknowledges Richard Wright at Idaho National Laboratory for technical support, as well as Joel Simpson for support maintaining and running laboratory equipment.

7. REFERENCES

1. Y. Yamamoto, P. J. Maziasz, P.J., and T.-L. Sham, *Report on the Optimization and Testing Results of Advanced Austenitic Alloys*, ORNL/TM-2012/401 (2012) Oak Ridge National Laboratory, Oak Ridge, TN.
2. J. Wright, T. Lillo, L. and Carroll, *Intermediate Term Creep-Fatigue Testing of Advanced Alloys*, INL/LTD-15-36013 (2015) Idaho National Laboratory, Idaho Falls, ID.
3. L. J. Carroll and J. K. Benz, *Intermediate-Term Creep-Fatigue Testing of Alloy 709 and Optimized Grade 92*, INL/LTD-14-33022 (2014) Idaho National Laboratory, Idaho Falls, ID.
4. L. J. Carroll and J. K. Benz, *Intermediate-Term Creep-Fatigue Testing of an Advanced Austenitic Alloy*, INL/LTD-13-30219 (2013) Idaho National Laboratory, Idaho Falls, ID.
5. L. J. Carroll, and M. C. Carroll, *Creep-Fatigue Behavior of Advanced Alloys*, INL/LTD-12-26862 Rev. 1 (2012) Idaho National Laboratory, Idaho Falls, ID.
6. L. J. Carroll and J. K. Benz, *Intermediate-Term Creep-Fatigue Testing of an Advanced Austenitic Alloy*, INL/EXT-13-30219 (2013) Idaho National Laboratory, Idaho Falls, ID.
7. M. C. Carroll, and M. C. Carroll, *Creep-Fatigue Behavior of Advanced Alloys*, INL/LTD-12-26862 Rev. 1 (2012) Idaho National Laboratory, Idaho Falls, ID.
8. M. McMurtrey, L. Carroll, and J. Wright, *Microstructural Effects on Creep-Fatigue Life of Alloy 709*, INL/EXT-17-41079 (2017) Idaho National Laboratory, Idaho Falls, ID.
9. L. Tan, Y. Yamamoto, and T.-L. Sham, *Materials Procurement and Related Examinations of Advanced Ferritic-Martensitic and Austenitic Alloys*, ORNL/TM-2013/325 (2013) Oak Ridge National Laboratory, Oak Ridge, TN.
10. "Creep Fatigue Testing," PLN-3346, Revision 9, (2017) INL/MIS-10-18953.
11. ASTM International, "Standard Test Method for Strain-Controlled Fatigue Testing," E606-12 (2012).
12. ASTM International, "Standard Test Method for Creep-Fatigue Testing," E2714-13 (2013).
13. "Creep Testing," PLN-3386 Revision 2, (2016) INL/MIS-16-40783.
14. ASTM International, "Standard Test Methods for Conducting Creep, Creep-Rupture, and Stress-Rupture Tests of Metallic Materials," E139-11 (2011).